Korean Journal of Radiology

KJR

Check for updates

Prevalence of Decreased Myocardial Blood Flow in Symptomatic Patients with Patent Coronary Stents: Insights from Low-Dose Dynamic CT Myocardial Perfusion Imaging

Yuehua Li, MD[1]*, Mingyuan Yuan, MD[2]*, Mengmeng Yu, MD[1], Zhigang Lu, MD[3], Chengxing Shen, MD[3], Yining Wang, MD[4], Bin Lu, MD[5], Jiayin Zhang, MD[1]

[1]Institute of Diagnostic and Interventional Radiology, Shanghai Jiao Tong University Affiliated Sixth People's Hospital, Shanghai, China; [2]Department of Radiology, Affiliated Zhoupu Hospital, Shanghai University of Medicine and Health Science, Shanghai, China; [3]Department of Cardiology, Shanghai Jiao Tong University Affiliated Sixth People's Hospital, Shanghai, China; [4]Department of Radiology, Peking Union Medical College Hospital, Chinese Academy of Medical Science & Peking Union Medical College, Beijing, China; [5]Department of Radiology, Fuwai Hospital, State Key Laboratory of Cardiovascular Disease, National Centre for Cardiovascular Diseases, Chinese Academy of Medical Sciences and Peking Union Medical College, Beijing, China

Objective: To study the prevalence and clinical characteristics of decreased myocardial blood flow (MBF) quantified by dynamic computed tomography (CT) myocardial perfusion imaging (MPI) in symptomatic patients without in-stent restenosis.
Materials and Methods: Thirty-seven (mean age, 71.3 ± 10 years; age range, 48–88 years; 31 males, 6 females) consecutive symptomatic patients with patent coronary stents and without obstructive *de novo* lesions were prospectively enrolled to undergo dynamic CT-MPI using a third-generation dual-source CT scanner. The shuttle-mode acquisition technique was used to image the complete left ventricle. A bolus of contrast media (50 mL; iopromide, 370 mg iodine/mL) was injected into the antecubital vein at a rate of 6 mL/s, followed by a 40-mL saline flush. The mean MBF value and other quantitative parameters were measured for each segment of both stented-vessel territories and reference territories. The MBF$_{ratio}$ was defined as the ratio of the mean MBF value of the whole stent-vessel territory to that of the whole reference territory. An MBF$_{ratio}$ of 0.85 was used as the cut-off value to distinguish hypoperfused from non-hypoperfused segments.
Results: A total of 629 segments of 37 patients were ultimately included for analysis. The mean effective dose of dynamic CT-MPI was 3.1 ± 1.2 mSv (range, 1.7–6.3 mSv). The mean MBF of stent-vessel territories was decreased in 19 lesions and 81 segments. Compared to stent-vessel territories without hypoperfusion, the mean MBF and myocardial blood volume were markedly lower in hypoperfused stent-vessel territories (77.5 ± 16.6 mL/100 mL/min vs. 140.4 ± 24.1 mL/100 mL/min [$p <$ 0.001] and 6.4 ± 3.7 mL/100 mL vs. 11.5 ± 4 mL/100 mL [$p <$ 0.001, respectively]). Myocardial hypoperfusion in stent-vessel territories was present in 48.6% (18/37) of patients. None of clinical parameters differed statistically significantly between hypoperfusion and non-hypoperfusion subgroups.
Conclusion: Decreased MBF is commonly present in patients who are symptomatic after percutaneous coronary intervention,

despite patent stents and can be detected by dynamic CT-MPI using a low radiation dose.

Keywords: *Coronary artery disease; Multidetector computed tomography; Angiography; Stents; Percutaneous coronary intervention*

INTRODUCTION

Percutaneous coronary intervention (PCI) is currently a key strategy for myocardial revascularization in patients with obstructive coronary artery disease (1, 2). In the era of drug-eluting stents, the incidence of in-stent restenosis (ISR) has decreased markedly compared to that with bare metal stents (3-5). However, it is not uncommon for post-PCI patients to have angina or atypical chest pain, even with patent stents. According to previous invasive coronary angiography (ICA) studies, microvascular dysfunction (MVD) has been found in approximately 50% of symptomatic post-PCI patients with patent stents (6, 7).

With the recent introduction of third-generation dual-source computed tomography (CT) scanners, coronary CT angiography (CCTA) has been revealed to be accurate for the diagnosis of ISR of both large and small caliber stents (8). However, it is a purely anatomical method, which lacks functional information. Positron emission tomography (PET) perfusion imaging is currently the best functional imaging modality for non-invasive quantitative evaluation of myocardial ischemia and MVD (9-12). Similar to PET imaging, dynamic CT myocardial perfusion imaging (MPI) by third-generation dual-source CT can also evaluate various quantitative perfusion parameters, allowing accurate assessment of myocardial ischemia with reference to invasive fractional flow reserve or cardiac magnetic resonance (CMR)-MPI (13-15). However, the value of this novel imaging modality for the assessment of post-PCI patients with angina and patent stents has not been explored to date. We hypothesized that myocardial blood flow (MBF) quantified by dynamic CT-MPI might facilitate diagnosis of post-PCI-MVD. Therefore, we investigated the prevalence of decreased MBF quantified by dynamic CT-MPI in symptomatic patients without ISR. In addition, we also studied differences in clinical characteristics between patients with and without hypoperfused myocardial segments.

MATERIALS AND METHODS

Patient Population

Between November 2016 and April 2018, consecutive symptomatic post-PCI patients with exertional angina or chest discomfort were prospectively enrolled. The inclusion criterion was that stent patency was confirmed by either CCTA (if stent calibers were ≥ 3 mm and stent images contained no artifacts) or ICA (if stent calibers were < 3 mm or CCTA images contained artifacts). Exclusion criteria were as follows: 1) Significant ISR (defined as diameter stenosis ≥ 50%), confirmed by either CCTA or ICA; 2) concomitant obstructive native coronary lesions (defined as diameter stenosis ≥ 50%); 3) previous history of myocardial infarction according to medical records; 4) previous history of cardiomyopathies; 5) usage of adenosine triphosphate contraindicated. All recruited patients were referred for stress dynamic CT-MPI for evaluation of myocardial perfusion. All patients signed written informed consent, and the study protocol was approved by the ethics committee of the hospital. One-hundred-and-thirty-three post-PCI patients were initially included on the basis of the
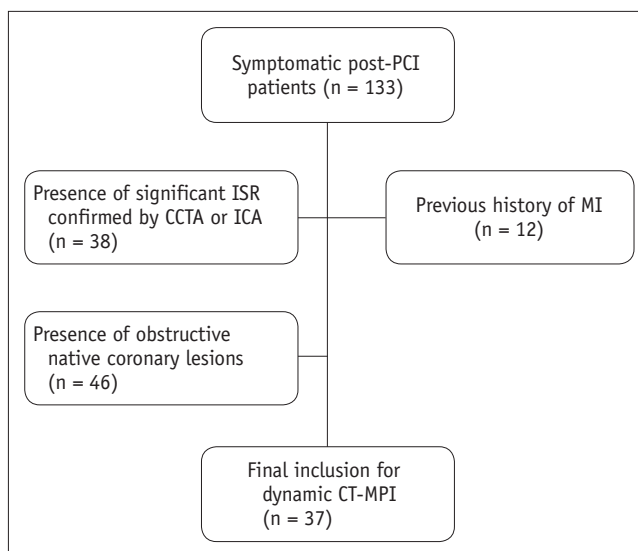

Fig. 1. Flowchart illustrating inclusion and exclusion criteria.
CCTA = coronary CT angiography, CT = computed tomography, ICA = invasive coronary angiography, ISR = in-stent restenosis, MI = myocardial infarction, MPI = myocardial perfusion imaging, PCI = percutaneous coronary intervention

presence of recurrent angina or chest discomfort. However, 38 patients were then excluded due to the presence of significant ISR, whereas another 12 patients with a history of myocardial infarction were excluded. In addition, a further 46 patients were excluded due to obstructive native coronary lesions revealed by CCTA or ICA. Therefore, 37 patients (mean age, 71.3 ± 10 years; age range, 48–88 years; 31 males [mean age, 70.8 ± 9.6 years; age range, 48–88] and 6 females [mean age, 73.8 ± 12.7 years; age range, 53–88], $p = 0.504$) were finally included in our study (Fig. 1).

CT-MPI Protocol

A third-generation dual-source CT scanner (SOMATOM Force, Siemens Healthineers, Forchheim, Germany), equipped with a fully integrated circuit detector system (Stellar[Infinity], Siemens Healthineers) was employed for CT-MPI acquisition. All patients were instructed to refrain from caffeine intake 24 hours prior to the examination. The calcium score was used to calculate the calcification burden of each pericardial vessel. The scan range of dynamic CT-MPI was planned on the basis of calcium score images. Adenosine triphosphate (Guangdong South China Pharmaceutical Company, Guangdong, China) was infused over 3 minutes at 160 µg/kg/min before triggering the MPI acquisition. A bolus of contrast media (50 mL; iopromide, 370 mg iodine/mL, Bayer Healthcare, Berlin, Germany) was injected into the antecubital vein at a rate of 6 mL/s, followed by a 40-mL saline flush, using a dual-barrel power injector (Tyco, Cincinnati, OH, USA). CT-MPI examinations were started 5 seconds after initiating the contrast injection, using an axial scan mode triggered at 250 ms after the R wave (end-systole). Imaging the complete left ventricle required a shuttle-mode acquisition technique. By moving the table back and forth after each acquisition, 2 series of images were collected, which together covered the entire myocardium. Depending on heart rate, scans were performed every second or third heart cycle, resulting in a series of 10–15 phases acquired over a period of approximately 31 seconds. The acquired values of parameters of CT-MPI are listed as follows: collimation = 96 x 0.6 mm, reconstructed slice thickness = 3 mm, reconstructed slice interval = 2 mm, rotation time = 250 ms, tube voltage = 70 kVp, and effective tube current = 250 mAs.

Nitroglycerin was administered sublingually in all patients prior to CCTA. CCTA was performed 5 minutes after CT-MPI by using a bolus tracking technique, with regions of interest placed in the ascending aorta. A bolus of contrast media was injected into antecubital vein at a rate of 4–5 mL/s, followed by a 40-mL saline flush, by using a dual-barrel power injector. Prospective electrocardiography-triggered sequential acquisition was carried out in all patients undergoing CCTA, with the center of the triggering window set at diastole or systole, depending on the heart rate, with collimation = 96 x 0.6 mm, reconstructed slice thickness = 0.75 mm, reconstructed slice interval = 0.5 mm, rotation time = 250 ms, and application of automated tube voltage and current modulation (CARE kV and CARE Dose 4D, Siemens Healthineers).

CT-MPI Analysis

The CT-MPI data were reconstructed using a dedicated kernel for the reduction of iodine beam-hardening artifacts (Qr36) and analyzed using CT-MPI software (Myocardial perfusion analysis; VPCT body, Siemens Healthineers). Motion correction was applied where necessary to correct breathing-related misregistration of the left ventricle. For quantification of MBF, the influx of contrast medium was measured using the arterial input function (AIF). The AIF was sampled in the descending aorta by including both the cranial and caudal sections. For the quantification of MBF and other parameters, myocardial time-attenuation curves were coupled with AIF using a hybrid deconvolution model (16, 17).

For quantitative analysis, a region of interest (ROI) was manually placed to sample the MBF and other parameters on a segment base, using a 17-segment model (18). To ensure accurate matching of coronary distribution and associated myocardial territories, the patient-specific coronary anatomy on CCTA (right, left, or balanced dominance, length of left anterior descending coronary artery) was used to determine the precise segmentation in the short-axis view of the fused myocardial color-coded map. The ROI was drawn to cover the whole area suspected of having a perfusion defect, within the segment, or to cover the whole segment when a perfusion defect was absent. The short-axis view of the fused myocardial color-coded map was utilized for quantification of all segments, except for the apical segment, which was evaluated on the vertical long-axis view. The mean value of different quantitative parameters, including MBF, myocardial blood volume (MBV), time-to-peak (TTP), and tissue-transit time (TTT), were measured for each segment of both stented-vessel territories and reference territories. The MBF$_{ratio}$ was defined as the ratio of the mean MBF value of the whole stent-vessel territory to the mean

MBF value of the whole reference territory. Because previous CT-MPI studies have demonstrated that the global MBF value varies among patients (19), an MBF$_{ratio}$ of 0.85 was used as the cut-off value to distinguish hypoperfused from non-hypoperfused segments (20).

Two cardiovascular radiologists (observer 1 with 10 years of experience in cardiac imaging and observer 2 with 6 years of experience in cardiac imaging), who were blinded to patients' clinical history, independently analyzed all CT-MPI data. The mean values of quantitative parameters measured by the 2 observers were used for analysis. Any disagreement between the observers was resolved by consensus.

CCTA Image Reconstruction and Analysis

For better delineation of both the vessel wall and stent lumen, 2 sets of axial images were reconstructed with different kernels and strength levels using a third-generation iterative reconstruction technique (ADMIRE, Siemens Healthineers): smooth kernel (Bv40, strength 3) and sharp kernel (Bv44, strength 4). Data were transferred to an offline workstation (Syngo.Via, Siemens Healthineers) for further analysis. Curved planar reformation and short-axis view of the stents, with sharp kernel reconstruction, were used for evaluation of ISR, whereas images with smooth kernel reconstruction were employed for the assessment of native coronary arteries.

ISR was assessed by CCTA (if stent calibers were ≥ 3 mm and stent images contained no artifacts) or ICA (if stent calibers were < 3 mm or CCTA images contained artifacts). Binary ISR was considered as an in-stent neointimal proliferation with diameter stenosis ≥ 50%. Obstructive native coronary lesions were defined as diameter stenosis ≥ 50% of at least 1 major epicardial coronary artery. Only the CT-MPI data of patients without binary ISR and obstructive native coronary stenosis were used for further analysis.

Statistical Analysis

Statistical analysis was performed sing MedCalc Statistical Software (ver. 15.2.2; MedCalc Software bvba, Ostend, Belgium). Quantitative variables were expressed as mean ± standard deviation. Interobserver agreement was expressed in Cohen's kappa value for categorical variables. One-sample Kolmogorov–Smirnov tests were used to check the assumption of normal data distribution. Student's t test was used for normally distributed data, and the Mann-Whitney U test was used for data that were not normally distributed.

Chi-square tests were used to compare proportions. P values < 0.05 were considered to indicate statistically significant differences.

RESULTS

Clinical Characteristics

The dose length product of dynamic CT-MPI was 218.2 ± 83.1 mGy*cm (range, 120–448 mGy*cm), corresponding to an effective dose of 3.1 ± 1.2 mSv (range, 1.7–6.3 mSv). The mean heart rates before and after the pharmaceutical stress was 67.3 ± 8.8 bpm and 80.3 ± 8.2 bpm, respectively (p < 0.001). The mean interval between previous PCI and dynamic CT-MPI was 31.4 ± 23.8 months (range, 3–92 months). Detailed demographic data are given in Table 1.

Myocardial Perfusion Parameters of Stent-Vessel Territories and Reference Territories

Here, 37 patients, with a total of 629 segments, were included for evaluation. There were 8 patients with 2 stented vessels. None of the patients had 3 stented vessels. Artifacts were absent from all segments in which final measurements were successfully performed. Among the 629 segments, 180 segments were assigned to 45 stent-vessel territories, while 449 segments were assigned as reference territories. Compared to reference territories, the overall mean MBF and MBV were significantly lower in stent-vessel territories, whereas the mean TTT and TTP were markedly

Table 1. Demographic Data

Population	37
Age (years)	71.3 ± 10
Risk factors (%)	
Hyperlipidemia	21 (56.8)
Hypertension	29 (78.4)
Smoking	18 (48.6)
Diabetes	19 (51.4)
Clinical presentations (%)	
Stable angina	29 (78.4)
Atypical chest pain	8 (21.6)
Stented vessel (n = 45) (%)	
LM	1 (2.2)
LAD	16 (35.6)
LCx	11 (24.4)
RCA	15 (33.3)
Diagonal	1 (2.2)
Ramus intermedius	1 (2.2)

LAD= left anterior descending, LCx= left circumflex, LM= left main, RCA= right coronary artery

Table 2. Quantitative Myocardial Perfusion Parameters in Stent-Vessel Territories and Reference Territories

All Segments (n = 629)	Stent-Vessel Territories (n = 180)	Reference Territories (n = 449)	P
MBF (mL/100 mL/min)	114.4 ± 37.7	140.4 ± 24.1	< 0.001
MBV (mL/100 mL)	9 ± 4.5	11.5 ± 4	< 0.001
TTT (s)	13.6 ± 2.3	12.1 ± 2	< 0.001
TTP (s)	15.6 ± 2.6	14.5 ± 2.6	< 0.001
Hypoperfused Stent Segments and Reference Segments (n = 530)*	Stent-Vessel Territories (n = 81)	Reference Territories (n = 449)	P
MBF (mL/100 mL/min)	77.5 ± 16.6	140.4 ± 24.1	< 0.001
MBV (mL/100 mL)	6.4 ± 3.7	11.5 ± 4	< 0.001
TTT (s)	14.6 ± 2.3	12.1 ± 2	< 0.001
TTP (s)	16.7 ± 2	14.5 ± 2.6	< 0.001
Non-Hypoperfused Stent Segments and Reference Segments (n = 548)†	Stent-Vessel Territories (n = 99)	Reference Territories (n = 449)	P
MBF (mL/100 mL/min)	144.5 ± 18.3	140.4 ± 24.1	0.104
MBV (mL/100 mL)	11.1 ± 4	11.5 ± 4	0.367
TTT (s)	12.8 ± 2	12.1 ± 2	0.002
TTP (s)	14.7 ± 2.6	14.5 ± 2.6	0.326

*All segments of stent-vessel territories with hypoperfusion (defined as $MBF_{stent}/MBF_{ref} \leq 0.85$). Reference territories included all segments of non-stented vessel territories, †All segments of stent-vessel territories without hypoperfusion (defined as $MBF_{stent}/MBF_{ref} > 0.85$). Reference territories included all segments of non-stented vessel territories. MBF = myocardial blood flow, MBF_{ref} = myocardial blood flow of reference territories, MBF_{stent} = myocardial blood flow of stent-vessel territories, MBV = myocardial blood volume, TTP = time-to-peak, TTT = tissue-transit time

longer (Table 2).

Incidence of Myocardial Hypoperfusion of Stent-Vessel Territories

According to lesion-based analysis, the mean MBF of stent-vessel territories was decreased in 19 lesions and 81 segments (defined as the ratio of MBF of stent territories versus MBF of reference territories less than 0.85). Compared to stent-vessel territories without hypoperfusion, the mean MBF and MBV in stent-vessel territories with hypoperfusion were markedly lower (77.5 ± 16.6 mL/100 mL/min vs. 140.4 ± 24.1 mL/100 mL/min and 6.4 ± 3.7 mL/100 mL vs. 11.5 ± 4 mL/100 mL, $p < 0.001$) (Figs. 2-4). Similarly, the mean TTT and TTP were also significantly longer for the hypoperfused segments (Table 2). In addition, the ratios of MBF_{stent}/MBF_{ref} and MBV_{stent}/MBV_{ref} were notably smaller for hypoperfused stent-vessel territories (Table 3). Overall, myocardial hypoperfusion of stent-vessel territories was present in 48.6% (18/37) of patients. Different clinical parameters and medication history were also compared between patients with and without hypoperfused stent segments, but no other parameters differed significantly between the 2 subgroups (Table 4).

DISCUSSION

This study demonstrated that decreased MBF was present in 45% (81/180) of stent-vessel segments in post-PCI patients experiencing angina despite having patent stents. Dynamic CT-MPI by third-generation dual-source CT was able to detect this impaired myocardial perfusion at low radiation dose.

PCI is the most commonly employed revascularization strategy used to restore blood flow in cases with obstructive coronary lesions. Although recurrent angina is typically caused by ISR, coronary MVD has also been described as a potential mechanism for angina in patients who have previously undergone stent, but without ISR (21). Peri-procedural myocardial injury is not uncommon and is typically caused by the occurrence of distal embolization during procedures (22). Consequently, despite the patency of coronary stents, microvascular perfusion may be reduced in a substantial portion of the perfusion territory of the treated coronary artery because distal embolization could trigger abnormalities at the microvasculature level (23). The current study employed stress dynamic CT-MPI to demonstrate the presence of decreased MBF in post-PCI patients with angina and without ISR; this has not been reported previously. It is conceivable that the reduced

blood flow could be ascribed to the existence of MVD of stented-vessel territories, which is potentially caused by peri-procedural myocardial injury. This finding is in line with the result of a recent intracoronary electrocardiogram study, which revealed impaired microvascular perfusion after stent implantation in 36.9% of patients undergoing
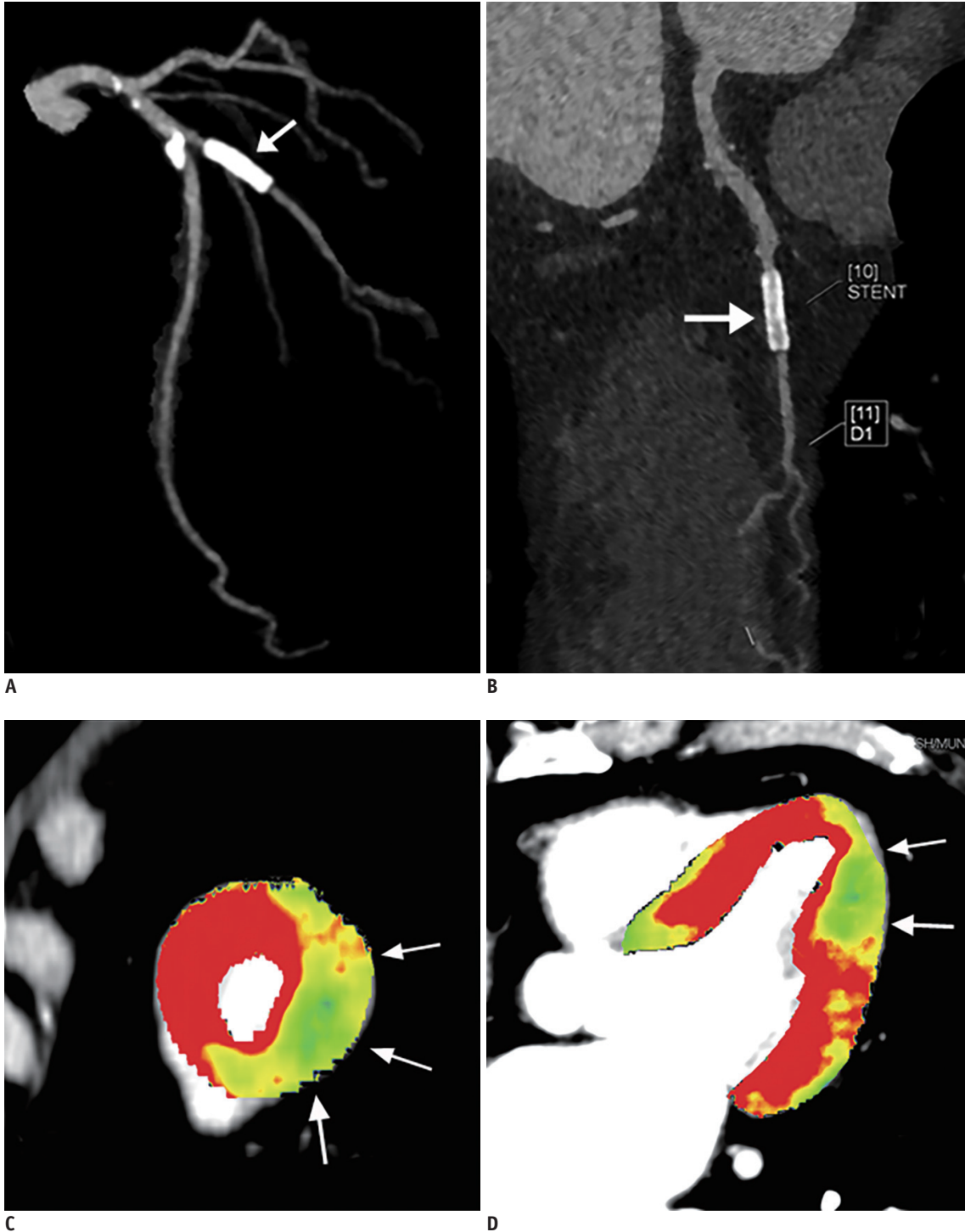

Fig. 2. Representative case of post-PCI patient with patent stent and reduced myocardial perfusion.
A. 3D-MIP image showed stent implantation of first diagonal branch (arrow). **B.** CPR image confirmed stent patency (arrow). **C.** Short-axis view of MBF fusion image revealing decreased MBF in apical lateral segment (arrows), corresponding to first diagonal branch territory. **D.** Long-axis view of MBF fusion image demonstrating decreased MBF in apical lateral segment (arrows); mean MBF was 90.5 mL/100 mL/min. CPR = curved planar reformation, MBF = myocardial blood flow, MIP = maximum intensity projection, 3D = three-dimensional
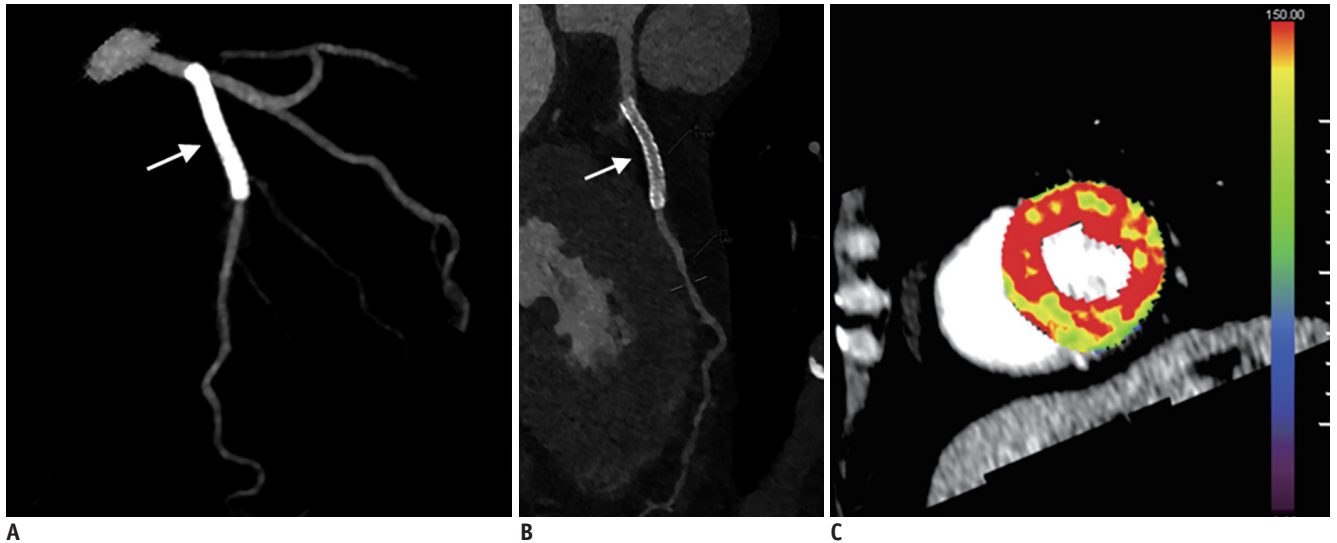
Fig. 3. Representative case of post-PCI patient with patent stent and normal myocardial perfusion.
A. 3D-MIP image showing stent implantation of proximal LAD (arrow). **B.** CPR image confirming stent patency (arrow). **C.** Short-axis view of MBF fusion image revealing normal MBF throughout left ventricle. Mean MBF of LAD territory was 150.9 mL/100 mL/min. LAD = left anterior descending
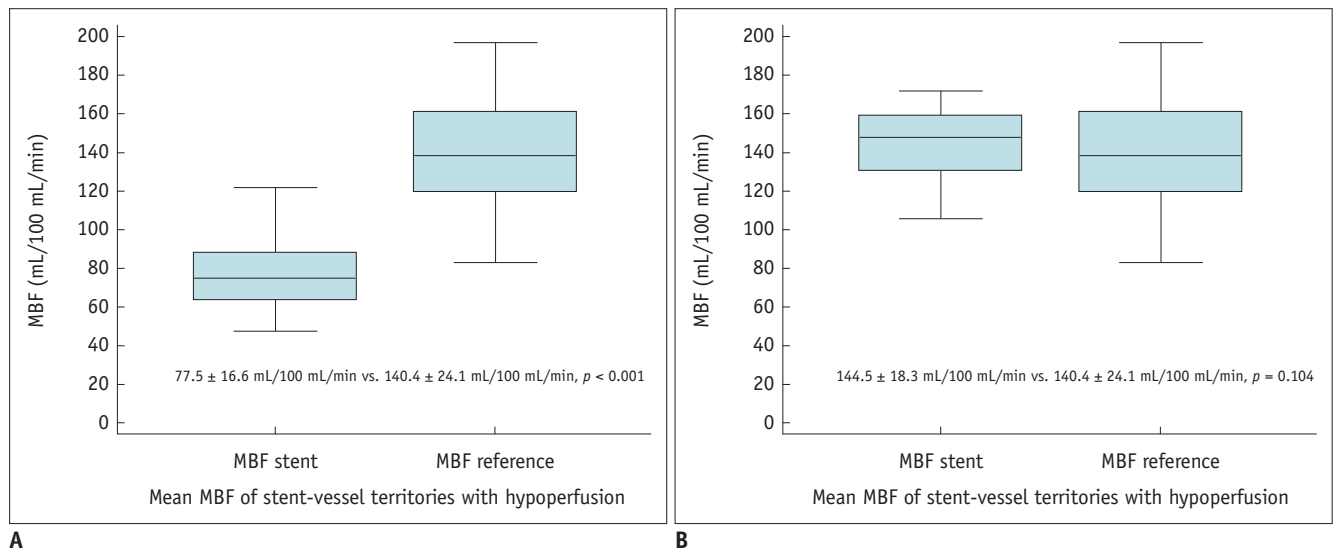

Fig. 4. Box plot of MBF for stent-vessel territories and reference territories.
A. Mean MBF of stent-vessel territories with hypoperfusion was significantly lower than that of reference territories. **B.** Mean MBF of stent-vessel territories with hypoperfusion was similar to that of that reference territories.

elective PCI (24). Furthermore, the present study also revealed that there was no significant difference in clinical risk factors and symptoms between MBF-reduced and MBF-preserved subgroups. This indicates that dynamic CT-MPI might be a more useful method than traditional clinical parameters for identifying potential MVD in symptomatic patients with patent stents. Therefore, the most important potential clinical implication of the current study lies in the classification of symptomatic patients without obstructive ISR. When decreased MBF is present in such a cohort,

further invasive tests, such as coronary flow reserve testing, might be warranted to confirm the diagnosis of MVD in order to optimize treatment strategy.

Additionally, the radiation dose of dynamic CT-MPI by third-generation dual-source CT was notably low, at a mean level of 3.1 mSv. Radiation exposure is a major concern of dynamic CT-MPI, which requires multiple acquisitions for the generation of time-attenuation curves. The average effective dose of dynamic CT-MPI was 9.23 mSv, according to previously published studies (19). Although this rate is

Table 3. Ratios of Different Parameters of Stent-Vessel Territories Versus Those of Reference Territories

	All Stent-Vessel Territories (n = 45)	Stent-Vessel Territories with Hypoperfusion (n = 19)	Stent-Vessel Territories without Hypoperfusion (n = 26)	P
MBF_{ratio}	0.82 ± 0.20	0.61 ± 0.11	0.98 ± 0.04	< 0.001
MBV_{ratio}	0.74 ± 0.22	0.53 ± 0.17	0.89 ± 0.11	< 0.001
TTT_{ratio}	1.10 ± 0.18	1.16 ± 0.21	1.06 ± 0.15	0.074
TTP_{ratio}	1.11 ± 0.13	1.15 ± 0.14	1.08 ± 0.11	0.072

Table 4. Comparison of Clinical Features between Patients with and without Hypoperfused Stent Segments

Clinical Parameters and Medication History	Patients with Hypoperfused Stent Segments (n = 18)	Patients without Hypoperfused Stent Segments (n = 19)	P
Clinical symptoms (%)			
Stable angina	15 (83.3)	14 (73.7)	0.693
Atypical chest pain	3 (16.7)	5 (26.3)	0.693
Hyperlipidemia (%)	11 (61.1)	10 (52.5)	0.743
Hypertension (%)	13 (72.2)	16 (84.2)	0.447
Smoking (%)	10 (55.6)	8 (42.1)	0.517
Diabetes (%)	12 (66.7)	7 (36.8)	0.103
Use of drugs (%)			
Use of β-blocker	14 (77.8)	16 (84.2)	0.693
Use of ACE-I	10 (55.6)	12 (63.2)	0.743
Use of nitrates	5 (27.8)	7 (36.8)	0.728
Use of statin	11 (61.1)	10 (52.6)	0.426
Use of calcium channel blockers	4 (22.2)	5 (26.3)	1.000
Use of aspirin	18 (100)	19 (100)	1.000
Use of clopidogrel	18 (100)	19 (100)	1.000

ACE-I = angiotensin-converting enzyme inhibitors

comparable to nuclear MPI (25), it is significantly higher than CCTA studies when multiple dose-reduction techniques are employed (26, 27). In the present study, the tube voltage and effective current were fixed to 70 kVp and 250 mAs, respectively, for dynamic perfusion imaging, regardless of patients' heart rate or body habitus. This makes the radiation dose of dynamic CT-MPI comparable to that of a routine CCTA.

Another clinical implication of the current findings is that the decreased MBF in post-PCI patients does not necessarily pertain to ISR. CT-MPI has previously been reported to have incremental value to CCTA for diagnosing ISR (28). The presence of a perfusion defect was considered as an indirect sign, indicating compromised stent patency. However, based on the current findings, decreased MBF could also be commonly encountered in symptomatic patients with patent stents, which is in line with the findings of previous invasive studies (6, 7). Therefore, it is unreliable to determine stent patency solely according to the myocardial perfusion status of the stented-vessel territory.

Despite these novel findings, the present study had

several limitations. First, only symptomatic patients with patent stents were enrolled. Patients with significant ISR were directly referred to balloon angioplasty treatment, whereas patients without chest discomfort were not evaluated. Further studies are required to determine the myocardial perfusion status in both symptomatic and asymptomatic cohorts in order to determine whether reduced MBF of stent-vessel territories is related to patients' symptoms. Second, we were unable to compare the CT-MPI findings with those of PET or invasive tests. Further investigations are warranted to confirm the association between this decreased MBF and MVD. Finally, the current study excluded patients with previous myocardial infarction based on medical records rather than on CMR imaging. Therefore, occult myocardial infarction might have been overlooked, which also could lead to significantly reduced MBF within stented territories.

In conclusion, decreased MBF is commonly present in symptomatic post-PCI patients who have patent stents. Dynamic CT-MPI by third-generation dual-source CT is able to detect this impaired myocardial perfusion at a low

radiation dose.

Conflicts of Interest

The authors have no potential conflicts of interest to disclose.

ORCID iDs

Jiayin Zhang
https://orcid.org/0000-0001-7383-7571
Yuehua Li
https://orcid.org/0000-0002-6511-8929
Mingyuan Yuan
https://orcid.org/0000-0002-6950-2864

REFERENCES

1. Sousa JE, Serruys PW, Costa MA. New frontiers in cardiology: drug-eluting stents: part I. *Circulation* 2003;107:2274-2279

2. Sousa JE, Serruys PW, Costa MA. New frontiers in cardiology: drug-eluting stents: part II. *Circulation* 2003;107:2383-2389

3. Moses JW, Leon MB, Popma JJ, Fitzgerald PJ, Holmes DR, O'Shaughnessy C, et al. Sirolimus-eluting stents versus standard stents in patients with stenosis in a native coronary artery. *N Engl J Med* 2003;349:1315-1323

4. Stone GW, Ellis SG, Cox DA, Hermiller J, O'Shaughnessy C, Mann JT, et al. A polymer-based, paclitaxel-eluting stent in patients with coronary artery disease. *N Engl J Med* 2004;350:221-231

5. Dangas GD, Claessen BE, Caixeta A, Sanidas EA, Mintz GS, Mehran R. In-stent restenosis in the drug-eluting stent era. *J Am Coll Cardiol* 2010;56:1897-1907

6. Hokimoto S, Tabata N, Yamanaga K, Sueta D, Akasaka T, Tsujita K, et al. Prevalence of coronary macro- and micro-vascular dysfunctions after drug-eluting stent implantation without in-stent restenosis. *Int J Cardiol* 2016;222:185-194

7. Ong P, Athanasiadis A, Perne A, Mahrholdt H, Schäufele T, Hill S, et al. Coronary vasomotor abnormalities in patients with stable angina after successful stent implantation but without in-stent restenosis. *Clin Res Cardiol* 2014;103:11-19

8. Li Y, Yu M, Li W, Lu Z, Wei M, Zhang J. Third generation dual-source CT enables accurate diagnosis of coronary restenosis in all size stents with low radiation dose and preserved image quality. *Eur Radiol* 2018;28:2647-2654

9. Gould KL, Johnson NP, Bateman TM, Beanlands RS, Bengel FM, Bober R, et al. Anatomic versus physiologic assessment of coronary artery disease. Role of coronary flow reserve, fractional flow reserve, and positron emission tomography imaging in revascularization decision-making. *J Am Coll Cardiol* 2013;62:1639-1653

10. El Fakhri G, Kardan A, Sitek A, Dorbala S, Abi-Hatem N, Lahoud Y, et al. Reproducibility and accuracy of quantitative myocardial blood flow assessment with (82) Rb PET: comparison with (13)N-ammonia PET. *J Nucl Med* 2009;50:1062-1071

11. Alexánderson E, Ochoa JM, Calleja R, Juárez-Rojas JG, Prior JO, Jácome R, et al. Endothelial dysfunction in systemic lupus erythematosus: evaluation with 13N-ammonia PET. *J Nucl Med* 2010;51:1927-1931

12. Recio-Mayoral A, Rimoldi OE, Camici PG, Kaski JC. Inflammation and microvascular dysfunction in cardiac syndrome X patients without conventional risk factors for coronary artery disease. *JACC Cardiovasc Imaging* 2013;6:660-667

13. Bamberg F, Becker A, Schwarz F, Marcus RP, Greif M, von Ziegler F, et al. Detection of hemodynamically significant coronary artery stenosis: incremental diagnostic value of dynamic CT-based myocardial perfusion imaging. *Radiology* 2011;260:689-698

14. Bamberg F, Marcus RP, Becker A, Hildebrandt K, Bauner K, Schwarz F, et al. Dynamic myocardial CT perfusion imaging for evaluation of myocardial ischemia as determined by MR imaging. *JACC Cardiovasc Imaging* 2014;7:267-277

15. Coenen A, Rossi A, Lubbers MM, Kurata A, Kono AK, Chelu RG, et al. Integrating CT myocardial perfusion and CT-FFR in the work-up of coronary artery disease. *JACC Cardiovasc Imaging* 2017;10:760-770

16. Bamberg F, Klotz E, Flohr T, Becker A, Becker CR, Schmidt B, et al. Dynamic myocardial stress perfusion imaging using fast dual-source CT with alternating table positions: initial experience. *Eur Radiol* 2010;20:1168-1173

17. Rossi A, Merkus D, Klotz E, Mollet N, de Feyter PJ, Krestin GP. Stress myocardial perfusion: imaging with multidetector CT. *Radiology* 2014;270:25-46

18. Cerqueira MD, Weissman NJ, Dilsizian V, Jacobs AK, Kaul S, Laskey WK, et al.; American Heart Association Writing Group on Myocardial Segmentation and Registration for Cardiac Imaging. Standardized myocardial segmentation and nomenclature for tomographic imaging of the heart. A statement for healthcare professionals from the Cardiac Imaging Committee of the Council on Clinical Cardiology of the American Heart Association. *Circulation* 2002;105:539-542

19. Danad I, Szymonifka J, Schulman-Marcus J, Min JK. Static and dynamic assessment of myocardial perfusion by computed tomography. *Eur Heart J Cardiovasc Imaging* 2016;17:836-844

20. Kono AK, Coenen A, Lubbers M, Kurata A, Rossi A, Dharampal A, et al. Relative myocardial blood flow by dynamic computed tomographic perfusion imaging predicts hemodynamic significance of coronary stenosis better than absolute blood flow. *Invest Radiol* 2014;49:801-807

21. Monnink SH, Tio RA, Veeger NJ, Amoroso G, van Boven AJ, van Gilst WH. Exercise-induced ischemia after successful percutaneous coronary intervention is related to distal coronary endothelial dysfunction. *J Investig Med* 2003;51:221-226

22. Balian V, Galli M, Marcassa C, Cecchin G, Child M, Barlocco F, et al. Intracoronary ST-segment shift soon after elective percutaneous coronary intervention accurately predicts periprocedural myocardial injury. *Circulation* 2006;114:1948-

1954

23. Jaffe R, Dick A, Strauss BH. Prevention and treatment of microvascular obstruction related myocardial injury and coronary no-reflow following percutaneous coronary intervention: a systematic approach. *JACC Cardiovasc Interv* 2010;3:695-704

24. Ikenaga H, Kurisu S, Nakao T, Kono S, Sumimoto Y, Watanabe N, et al. Predictive value of plaque morphology assessed by frequency-domain optical coherence tomography for impaired microvascular perfusion after elective stent implantation: the intracoronary electrocardiogram study. *Eur Heart J Cardiovasc Imaging* 2018;19:310-318

25. Einstein AJ, Moser KW, Thompson RC, Cerqueira MD, Henzlova MJ. Radiation dose to patients from cardiac diagnostic imaging. *Circulation* 2007;116:1290-1305

26. Zhang LJ, Wang Y, Schoepf UJ, Meinel FG, Bayer RR 2nd, Qi L, et al. Image quality, radiation dose, and diagnostic accuracy of prospectively ECG-triggered high-pitch coronary CT angiography at 70 kVp in a clinical setting: comparison with invasive coronary angiography. *Eur Radiol* 2016;26:797-806

27. Layritz C, Schmid J, Achenbach S, Ulzheimer S, Wuest W, May M, et al. Accuracy of prospectively ECG-triggered very low-dose coronary dual-source CT angiography using iterative reconstruction for the detection of coronary artery stenosis: comparison with invasive catheterization. *Eur Heart J Cardiovasc Imaging* 2014;15:1238-1245

28. Rief M, Zimmermann E, Stenzel F, Martus P, Stangl K, Greupner J, et al. Computed tomography angiography and myocardial computed tomography perfusion in patients with coronary stents: prospective intraindividual comparison with conventional coronary angiography. *J Am Coll Cardiol* 2013;62:1476-1485